Materials Research Proceedings **26** (2023) 337-342 https://doi.org/10.21741/9781644902431-55

Numerical strategies for modelling masonry arch bridges strengthened with PBO-FRCM composites

Enrico Compagnone[1, a], Salvatore Gazzo[2, b], Leopoldo Greco[2, c], Massimo Cuomo[2, d], Loredana Contrafatto[2, e *]

[1] Giniu Ingegneria e Architettura, Spinoff Università degli Studi di Catania, Italy

[2] Dipartimento di Ingegneria Civile e Architettura, Università degli Studi di Catania, Italy

[a]enrico.compagnone@giniu.it, [b]salvatore.gazzo@dica.unict.it, [c]leopoldo.greco@unict.it, [d]mcuomo@dica.unict.it, [e]loredana.contrafatto@unict.it

Keywords: Masonry Arch Bridge, FRCM, PBO

Abstract. The work reports some numerical tests concerning the use of the Embedded Truss elements implemented in the Midas FEA NX software in modeling a specific FRCM reinforcement system for masonry structures. The efficacy of the finite element is demonstrated through the comparison of the numerical results with experimental results obtained by other authors relating both to the mechanical characterization of the FRCM system materials and to the response of masonry arch models. The Embedded Truss element appears to be promising for application to real large structures, such as masonry arch bridges of large span or multi-span masonry bridges.

Introduction

New reinforcement systems have recently been proposed for retrofitting of existing masonry structures, consisting of cementitious matrices reinforced by fiber networks (Fiber Reinforced Concrete Matrix). These materials have high strength and durability, higher compatibility with the masonry support than other polymeric matrix reinforcement systems, originally conceived for the reinforcement of reinforced concrete works. FRCM are therefore finding extensive use in civil, infrastructural and historical masonry structures. The design of the reinforcement intervention and ex-post verification of the strengthened structure require the modeling of the reinforcement system through the software commonly used in structural analysis. The need for a detailed model of the reinforcement, capable of adequately simulating the crisis mechanisms, is countered by the need for streamlined numerical models, which do not burden the non-linear calculation in terms of size of the problem and computation time. The paper concerns modeling methods of a specific type of FRCM with PBO mesh. The method is based on the FEM technology named Embedded Truss and implemented in Midas FEA NX software [1]. The purpose is the definition of an effective modeling methodology of the FRCM reinforcement, which is susceptible of application in the structural analysis of masonry multi-arched bridges, even with very large spans. The method, applied to a specific commercial product, allows the accurate simulation of experimental tests for the characterization of the Ruregold PBO-Mesh 22/22 system [2] and reproduce the response of fiber reinforced masonry arches. Non-linear analyses based on the Smeared Crack Model for the masonry support and for the matrix of the reinforcement are presented. Specific constitutive models are used to define the fibers behaviour and the support-reinforcement interface. Sensitivity analyses show the importance that certain constitutive parameters have on the numerical solution. The numerical results are compared with the experimental ones to validate the method.

FEM Modeling of FRCM composites in the analysis of reinforced structures by Embedded Truss elements

In the literature of the last 10 years there are some attempts to model FRCM reinforcements in FEM codes [3]. This study proposes the use of the Embedded Truss element, implemented in

Materials Research Proceedings **26** (2023) 337-342 https://doi.org/10.21741/9781644902431-55

Midas FEA NX software [1], for modeling the mesh of the FRCM composite. The element consists in a truss embedded in a matrix. The lattice, which represents the fibers, and the matrix are attributed distinct nonlinear constitutive behaviour that reproduce the phenomenological aspects typical of the two materials.

The input method, coordinate system, material property, etc. of the Embedded Truss elements are identical to those of the standard Truss elements. Embedded Truss elements are generally used to model structural elements such as anchors, nails, and rock bolts, which ignore flexural behavior.

The elements (Fig. 1a) do not require the sharing of discretization nodes (Fig. 1b) and are therefore convenient for modeling and analyzing systems with fiber networks embedded in a continuum (Fig. 1c). The parent element in which the truss system is incorporated can be a flat deformation element or a solid element. The parent element includes each node of the Embedded Truss element. A multipoint constraint is used to automatically constrain the nodal displacement of the Embedded Truss element to the internal displacement of the parent element.

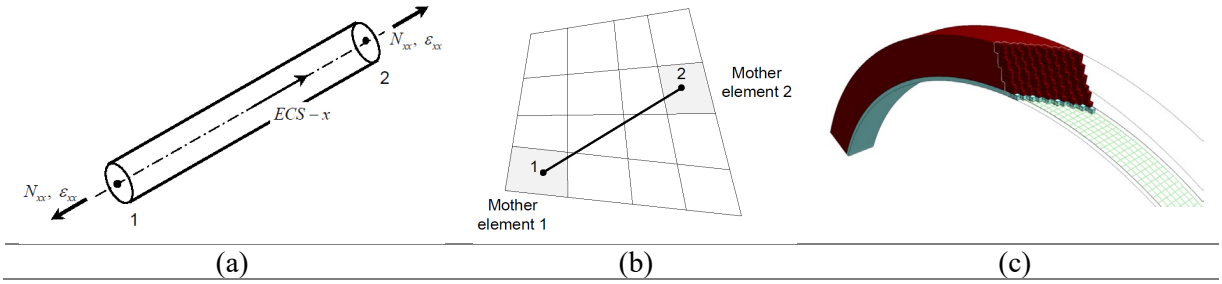

Figure 1 (a) Mother elements; (b) Embedded Truss element and (c) FEM model of a reinforced masonry arch

Both an elastic behaviour and a non-linear uniaxial constitutive behaviour with limited strength in compression and tension can be attributed to the Embedded Truss element.

The compressive non-linear behaviour of the matrix of the FRCM composite and of the masonry structure is ruled according to the Smeared Crack Model by a specific plasticity function. A Linearly Elastic-Perfectly Plastic stress-strain relationship defined by the elastic modulus E_{matrix} and compressive strength $f_{c,matrix}$ has been considered to model the FRCM matrix compressive behavior. A parabolic softening, defined by the size of the mesh h_{mesh}, the fracture energy $G_{c,matrix}$ and the compressive strength $f_{c,matrix}$ has been selected to define the compressive response of the masonry. The tensile behaviour is ruled by a crack detection surface. The FRCM matrix tensile behaviour is defined by Linear or Hordijk softening [1] defined by the size of the mesh h_{mesh}, the fracture energy $G_{f,matrix}$ and the tensile strength $f_{t,matrix}$. The tensile behaviour of the masonry is described by means of a bi-linear function defined by the size of the mesh h_{mesh}, the fracture energy $G_{f,masonry}$ and the tensile strength $f_{t,masonry}$. The shear behaviour of all fragile elements is defined by means of a linear τ-γ function, being β the coefficient regulating the slope.

Mechanical characterization of FRCM composites

The results of laboratory tests carried out on Ruregold PBO-Mesh 22/22 net, Ruregold MX-PBO mortar and on FRCM specimens reported in the work [4] have been considered for comparison.

Based on these experimental results, different numerical models have been calibrated for the various materials constituting the FRCM composite and for the composite itself.

Numerical results of the simulation of the uniaxial tensile test on a network specimen of PBO-Mesh 22/22 (Fig. 2a) are reported in the stress-strain graph shown in Fig. 2b. The net model is made of standard truss elements whose tensile behaviour is ruled by an elastoplastic function. Parameters of elastic modulus E =306924 [Mpa], tensile strength σ_t = 3031 [Mpa] and compressive strength σ_c = 0 [Mpa] allows a very good fitting of the experimental test.

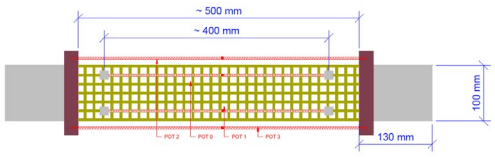

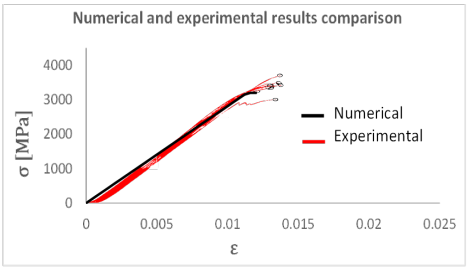

(a) (b)

Figure 2 (a) PBO mesh 22/22 specimen scheme and (b) Numerical and experimental result comparison

A second numerical test refers to the experimental tensile test on the FRCM composite panel reported in Fig. 3a [4]. The finite element model is illustrated in Figs. 3b, 3c, 3d.

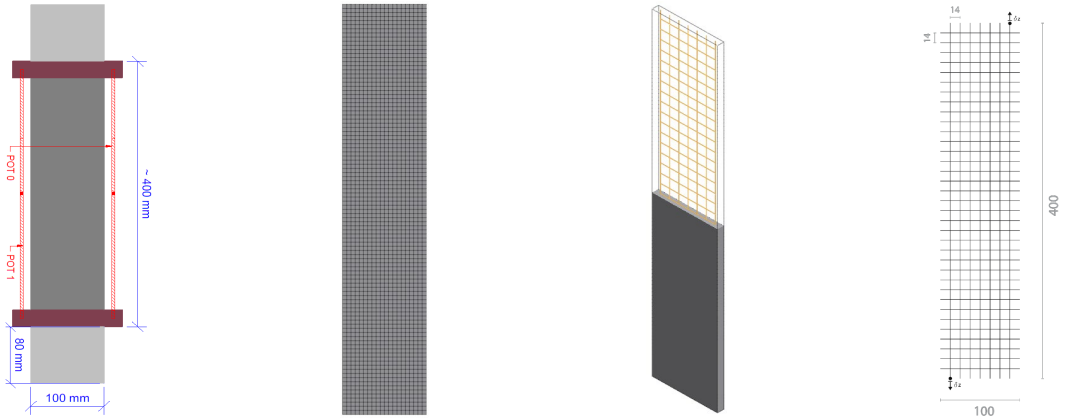

(a) (b) (c) (d)

Figure 3 (a) Geometric Scheme of FRCM Specimen; FRCM panel: FEM model (b) Frontal view, (c) cut plane Z and (d) the net.

The result of the numerical simulation is compared with the envelope of the stress-strain curves derived from the experimental tensile tests performed on 14 specimens of fiber-reinforced panels [4], according to the set-up shown in Fig. 3a. In Fig. 4 it is possible to appreciate the influence of the value of the fracture energy that defines the tensile behavior of the matrix of the FRCM system, governed by the linear softening. The matrix parameters are: elastic modulus E_{matrix} =2875 MPa, tensile strength $f_{t,matrix}$=2.84 MPa , fracture energy $G_{f,matrix}$ =0.05 N/mm.

A final test concerns the phenomenon of detachment of the FRCM from the support. Fig. 5a shows the discrete model. The dimensions of the surface of the reinforcement adhered to the tuff block are 100 x 300 mm. The longitudinal fibers of the mesh are extended to a length of 150 mm and then connected to a rigid bar. An interface has been introduced between the matrix and the support (in tuff), which approximates the stress redistribution in the matrix. Fig. 5 shows respectively the solid stress of all solid elements (b), the tangential tension along the interface (c) and the crack status at the interface (d) at a rate of the load of 85 %. It is clear that the detachment of the interface in the upper part involves a redistribution of the stresses in the matrix. The plot in Fig. 5a show that the loss of the interface bond strength happens about at the maximum force applied in experimental tests. The model based on the Embedded Truss is therefore able to adequately reproduce both the tensile response of the composite system and delamination tests, provided appropriate interface laws are adopted to simulate the behavior between the support and the matrix.

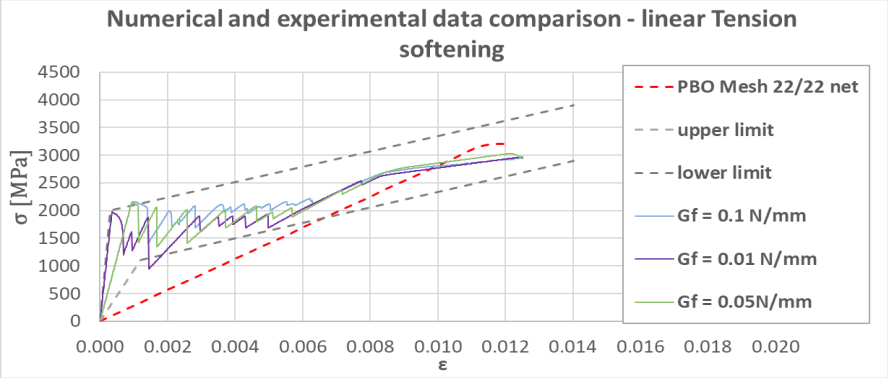

Figure 4 Comparison of numerical ad experimental results.

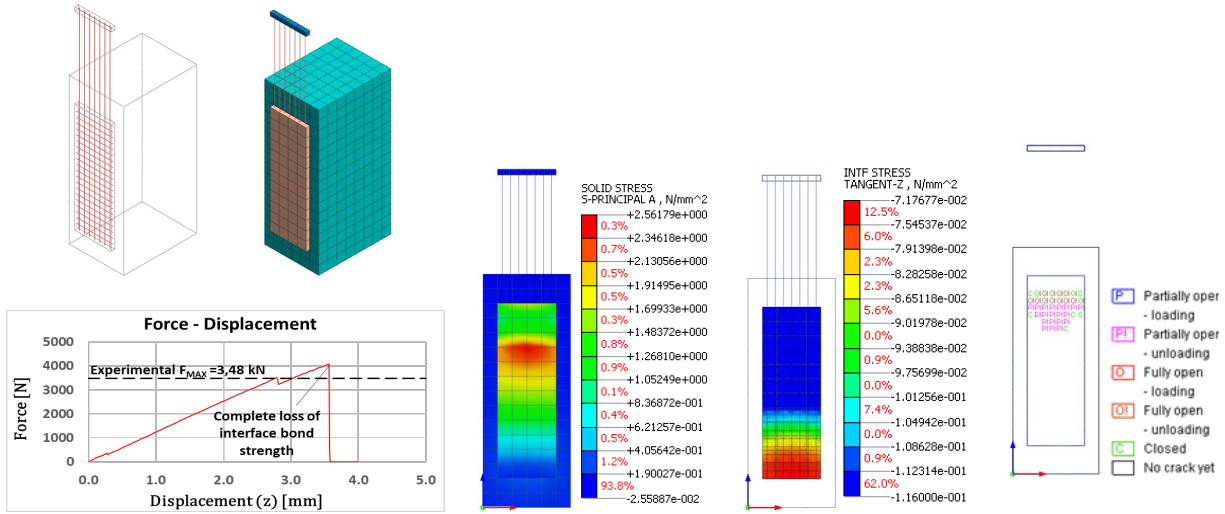

(a) (b) (c) (d)

Figure 5 Debonding FEM model. (a) Wireframe view, Solid View and Interface resistance; Results at 85% max load: (b) Matrix tensile stress; (c) Interface tangential stress and (d) Matrix crack status.

Behaviour of a single span FRCM strengthened masonry arch. Results and discussion.

In order to validate the proposed numerical technique, the experiments developed in [5] [6] [7] have been considered as benchmark test. The works experimentally investigate the structural behavior of masonry arches with different types of reinforcement, including PBO-Mesh 22/22 reinforcement. The tests were performed on 1:2 scale models with the dimensions depicted in Fig. 6a. The load is applied to a quarter of the span (378 mm from the left of the stump). Two samples were tested in the non-reinforced configuration (1-US and 2-US samples) and two samples with intrados reinforcement made of PBO Mesh 22/22 [5]; the control point of the displacements matches the loaded nodes. A nonlinear analysis was performed, in which the imposed displacement is assigned incrementally up to the last value of 6 mm with a step of 3.0 10^{-3}; the solution convergence criterion of the nonlinear problem was on the norm in energy (Work (W)) with a tolerance of 1. 0 10^{-3}. The elastic mechanical properties, from technical sheets and experimental identification, are reported in Table 1. The Smeared Crack model was used for both the matrix and the masonry. The input parameters of the non-linear model used in the numerical simulation were calibrated on the previous tests. Ruregold MX matrix: Linearly Elasic-Perfectly Plastic in compression, $f_{c,matrix}$= 26.4 MPa; Hordjik tensile softening, $f_{t,matrix}$= 2.64 MPa, $G_{f,matrix}$= 0.05 N/mm, internal length h_{mesh}=10 mm, shear retention factor β=0.01. Masonry: Linearly Elasic-

Perfectly Plastic in compression, $f_{c,masonry}$= 8.53 MPa; Linear tensile softening, $f_{t,masonry}$= 0.27 MPa, $G_{f,masonry}$= 0.001 N/mm, internal length h_{mesh} =20 mm, shear retention factor β=0.01.

Table 1 Material Parameters

	Ruregold MX-PBO	Masonry Parameter	PBO mesh 22-22
E (MPa)	7500	4500	270000
ν	0.3	0.27	0.3
G (MPa)	2885	1771.654	103846
f_t (MPa)			3031
ε_{el}			0.013

The graph in Fig. 6b shows the numerical response of both the unreinforced (N-UNR) and reinforced (N-RF) arch in terms of the Applied Force vs. Control Point Displacement curve. The model satisfactorily reproduces the experimental trend (Exp), both in the pre-peak and in the post-peak phase. In the case of the reinforced arch model, an increase of about 480% in the maximum strength was obtained compared to the non-reinforced model, in line with the experimental results.

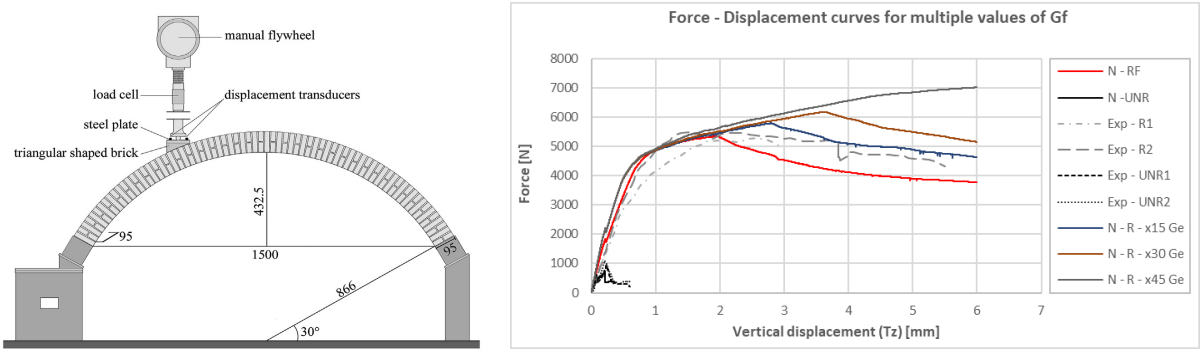

(a) (b)

Figure 6 (a) Geometric representation of the masonry arc specimen and (b) Comparison between experimental and numerical results of the strengthened and unstrengthened arch

In the graph (b), the three upper experimental curves (N-R) correspond to simulations in which the Hordjik tension function of the matrix was used with fracture energy $G_{f,matrix}$ chosen as multiple of the elastic energy E_e, that is, of the area underlying the strain curve in the elastic range. It is clear that, among the various parameters characterizing the Smeared Crack Model, the fracture energy plays a fundamental role and significantly affects the definition of the tensile behaviour of the matrix and the arch material. This implies that G_f must be carefully assessed. In the absence of certain data, the use of simpler models that adequately reproduce the salient aspects in the initial phase of the deformation history of the reinforced system, seems more prudential, even if they are not able to capture the entire evolutionary path of the damage.

From numerous numerical tests it has been observed that the shear retention function also plays a significant role, tuning the loss of shear stiffness (β G) and the evolutionary state of the cracks. On the contrary, not very significant, for the applications investigated, is the detailed definition of the compression damage function of both the masonry and the matrix of the FRCM. Indeed, the collapse mechanisms occur by the formation of hinges (cracks) due to the achievement of ultimate tensile stresses in specific sections, while the arch is divided into blocks whose compression stress state is well below the values at the elastic limit. For this reason, in the numerical applications, a simple Linearly Elastic-Perfectly Plastic model was assigned in compression to the brittle materials, that never exhibit excursions in the inelastic range.

The analysis of the crack pattern of the reinforced arch shows a widespread cracking in the masonry due to the transfer of the stresses performed by the FRCM, otherwise concentrated in the inelastic hinges in the case of the unreinforced arch.

(a) (b)

Figure 7 Crack pattern at the failure load of the unstrengthened arch (Tz=0.6 mm) (a) Unstrengthened arch and (b) strengthened arch

The above applications show the reliability of the numerical modeling methodology through Embedded Truss. The method appears suitable of application even to large structures, such as large-span and multi-span masonry arch bridges. Indeed, the reinforcement can be easily added to existent FEM models, with a limited increase of the size of the discrete structural model.

References

[1] MIDAS FEA NX, https://www.midasoft.com/

[2] RUREGOLD PBO-MESH 22/22, https://www.ruregold.com/it/

[3] D. V. Oliveira, B. Ghiassi, R. Allahvirdizadeh, X. Wang, G. Mininno e R. A. Silva, Macromodeling approach for pushover analysis of textile-reinforced mortar-strengthened masonry, Numerical Modeling of Masonry and Historical Structures (2019) 745-778. https://doi.org/10.1016/B978-0-08-102439-3.00021-X

[4] V. A. Alecci, F. Focacci, L. Rovero, G. Stipo e M. De Stefano, Extrados strengthening of brick masonry arches with PBO–FRCM composites: Experimental and analytical investigations, Composite Structures 149 (2016) 184-196. https://doi.org/10.1016/j.compstruct.2016.04.030

[5] V. A. Alecci, F. Focacci, L. Rovero, G. Stipo e M. De Stefano, Intrados strengthening of brick masonry arches with different FRCM composites: Experimental and analytical investigations, Composite Structures, 176 (2017) 898-909. https://doi.org/10.1016/j.compstruct.2017.06.023

[6] V. A. Alecci, G. Misseri, L. Rovero, G. Stipo, M. De Stefano, L. Feo e L. Raimondo, Experimental investigation on masonry arches strengthened with PBO-FRCM composite, Composites Part B, 100 (2016), 228-239. https://doi.org/10.1016/j.compositesb.2016.05.063

[7] E. Grande e G. Milani, Numerical simulation of the tensile behavior of FRCM strengthening systems, Composite, Composites Part B Engineering, 189 (2020) 107-886. https://doi.org/10.1016/j.compositesb.2020.107886